10

X-Ray Fluorescence

M. C. Miller

10.1 INTRODUCTION

The potential use of x rays for qualitative and quantitative elemental assay was appreciated soon after x rays were discovered. The early applications used Geiger-Mueller tubes and elaborate absorber arrays or crystal diffraction gratings to measure x rays. Later, advances in semiconductor detectors and associated electronics opened up the field of energy-dispersive x-ray fluorescence (XRF) analysis for general elemental assay.

XRF analysis is based on the fact that the x rays emitted from an ionized atom have energies that are characteristic of the element involved. The x-ray intensity is proportional to both the elemental concentration and the strength of the ionizing source. Photon ionization, which is achieved using either an x-ray tube or radioisotope, is most applicable to the nondestructive assay of nuclear material. Other methods of ionization are generally prohibitive because of the physical size and complexity of the ionization source.

XRF analysis is a complementary technique to densitometry (Chapter 9). Densitometry measures photons that are transmitted through the sample without interaction, whereas XRF measures the radiation produced by photons that interact within the sample. As indicated by Figure 10.1, densitometry is usually better suited for measuring samples with high concentrations of the element of interest, whereas XRF is the more useful technique for measuring samples with lower concentrations.

The literature on XRF analysis includes several general references (Refs. 1 through 4) that provide a thorough discussion of the method, with extensive bibliographies and information on attenuation correction procedures and both energy- and wavelength-dispersive XRF.

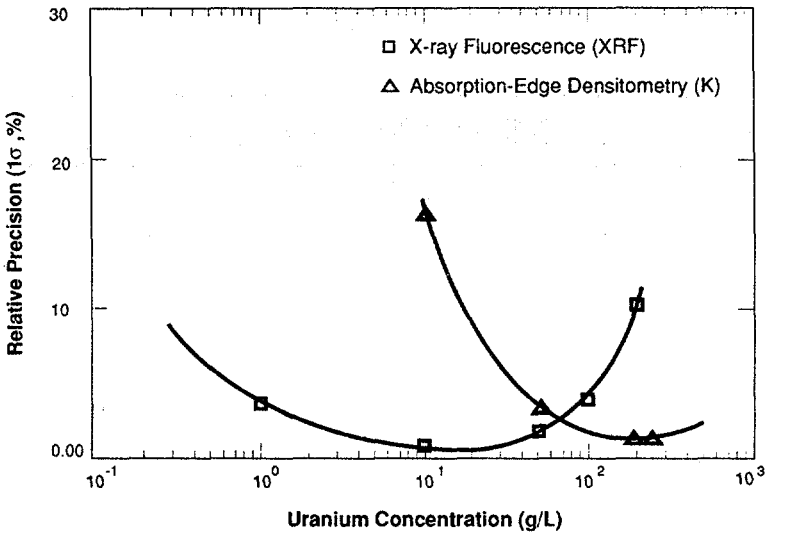

Fig. 10.1 *Solution assay precision vs uranium concentration for typical XRF measurements (squares) and absorption-edge densitometry measurements (triangles).*

10.2 THEORY

10.2.1 X-Ray Production

Section 1.3 of Chapter 1 contains a brief discussion of x-ray production. X rays originate from atomic electron transitions and are element-specific. In the stable atom, electrons occupy discrete energy levels that are designated (in order of decreasing binding energy) K, L_1, L_2, L_3, M_1, ..., M_5, N_1, ..., N_7, and so forth. The binding energy is the energy that must be expended to remove an electron from a given orbit. The vacancy thus created is filled by an electron from an outer orbit. The resultant loss in potential energy may appear as an x ray whose energy is equal to the difference in the binding energies of the two electron states. For example, if a uranium K electron is removed from the atom and an electron from the L_3 level falls into its place, the energy of the emitted x ray is 98.428 keV (115.591 keV minus 17.163 keV). The x ray produced by this transition is designated $K_{\alpha 1}$. The K-series x rays are produced by outer electrons filling a K-shell vacancy. Each x-ray transition has a specific probability or intensity. The K-to-L_3 transition is the most probable, and other intensities are usually expressed relative to $K_{\alpha 1}$. Figure 10.2 depicts the transitions involved in the production of the most abundant K and L x rays. Table 10-1 presents the major K and L lines of uranium and plutonium, along with their relative intensities. Figures 10.3 and 10.4 show the K and L x-ray spectra of uranium.

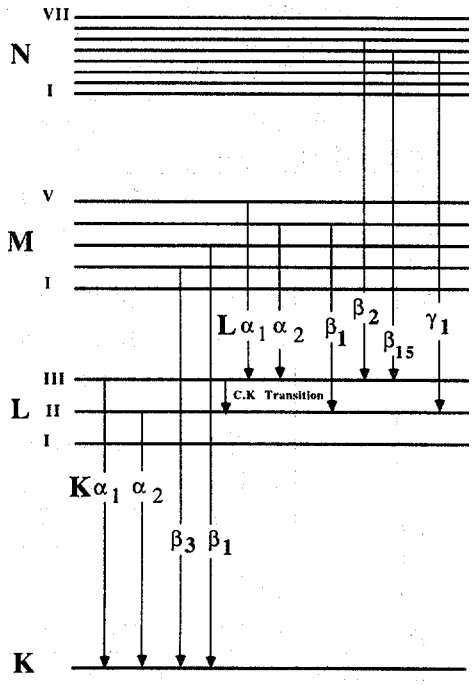

Fig. 10.2 Diagram of energy levels showing the atomic transitions that produce the major K and L x rays. (C.K. = Coster Krönig)

10.2.2 Fluorescence Yield

All ionizations do not result in x-ray emission. The Auger effect is a competing mechanism of atomic relaxation. In this process, the atom regains energy stability by emitting an outer shell electron. The ratio of the number of emitted x rays to the total number of ionizations is called the fluorescence yield ω_i, where i designates the shell involved. Fluorescence yield increases with atomic number and is greater than 95% for K x rays of elements with $Z > 78$ (see Figure 10.5). For a given element, the fluorescence yield decreases from the K series to the L and M series. The fluorescence yield can be approximated by (Ref. 1)

$$\omega_i = Z^4/(A_i + Z^4) \tag{10-1}$$

where A_i is approximately 10^6 for the K shell and 10^8 for the L shell.

10.2.3 Photon Transmission

For a photon to eject an electron, the photon energy must be greater than or equal to the electron binding energy. For example, to ionize K electrons of plutonium, the energy of the excitation photon must be at least 121.82 keV.

Table 10-1. Energies and relative intensities of the major K and L x rays of uranium and plutonium

Line	Transition (Final - Initial)	Energies in keV[a] Uranium (%)[b]	Plutonium (%)
$K_{\alpha 1}$	K - L_3	98.44 (100)	103.76 (100)
$K_{\alpha 2}$	K - L_2	94.66 (61.9)	99.55 (62.5)
$K_{\beta 1}$	K - M_3	111.31 (22.0)	117.26 (22.2)
$K_{\beta 3}$	K - M_2	110.43 (11.6)	116.27 (11.7)
$K_{\beta 2}$	K - $N_{2,3}$	114.34, 114.57 (12.3)	120.44, 120.70 (12.5)
$L_{\alpha 1}$	L_3 - M_5	13.62 (100)[c]	14.28 (100)
$L_{\alpha 2}$	L_3 - M_4	13.44 (10)	14.08 (10)
$L_{\beta 2}$	L_3 - N_5	16.43 (20)	17.26 (20)
L_{ι}	L_3 - M_1	11.62 (1-3)	12.12 (1-3)
$L_{\beta 1}$	L_2 - M_4	17.22 (50)	18.29 (50)
$L_{\gamma 1}$	L_2 - N_4	20.17 (1-10)	21.42 (1-10)
$L_{\beta 3}$	L_1 - M_3	17.45 (1-6)	18.54 (1-6)
$L_{\beta 4}$	L_1 - M_2	16.58 (3-5)	17.56 (3-5)

[a]Calculated from *Table of Isotopes*, Appendix III (L lines) (C. M. Lederer and V. S. Shirley, Eds., 7th ed. [John Wiley & Sons, Inc., New York, 1978]).
[b]Intensities relative to either $K_{\alpha 1}$ or $L_{\alpha 1}$ in percent.
[c]Approximate only (from Ref. 4).

The fraction of photons, F, that interact with the atomic electrons of a particular material is given by

$$F = 1 - \exp(-\mu\rho x) \tag{10-2}$$

where μ = mass attenuation coefficient
ρ = density of sample
x = thickness of sample.

If one plots the mass attenuation coefficient vs photon energy for a given element, sharp discontinuities (known as "absorption edges") are observed. Figure 10.6 shows the mass attenuation coefficient for uranium and plutonium. The edges indicate the sudden decrease in the photoelectric cross section for incident photon energies just below the binding energy of that particular electron state. The photoelectric interaction is the dominant process involved in photon-excited x-ray excitation.

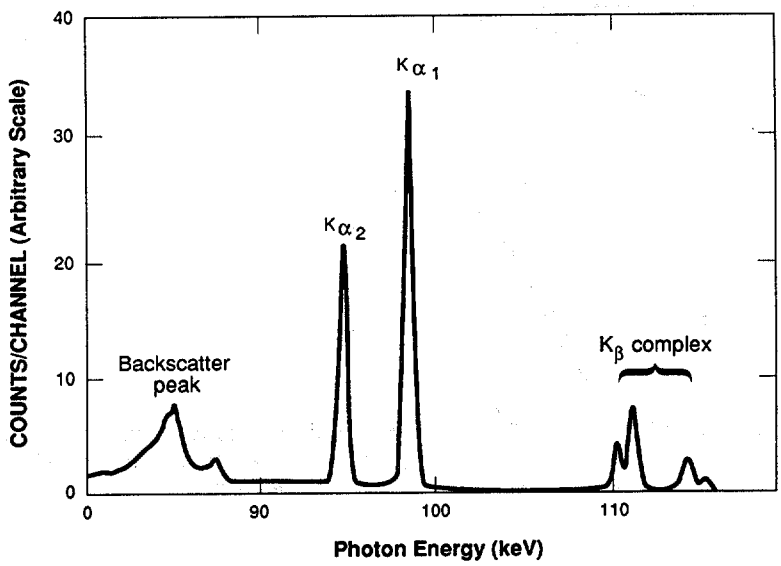

Fig. 10.3 *K x-ray spectrum of uranium. The excitation source is* ^{57}Co.

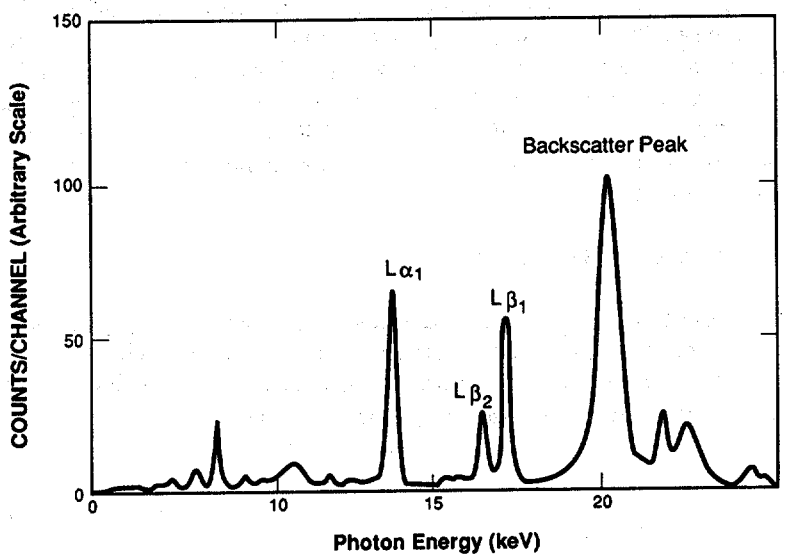

Fig. 10.4 *L x-ray spectrum of uranium. The excitation source is* ^{109}Cd.

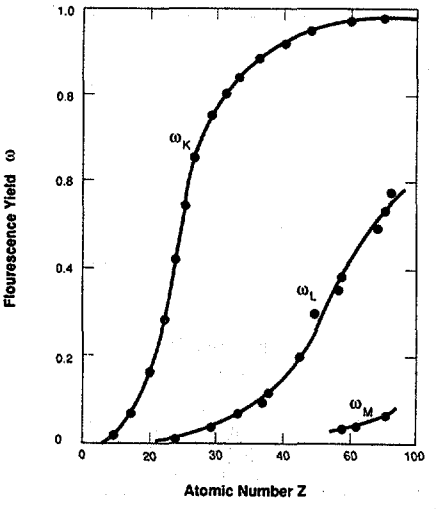

Fig. 10.5 Fluorescence yield for K, L, and M x rays as a function of atomic number.

Attenuation limits the sample size that can be analyzed by x-ray transmission techniques. Figure 10.7 shows the mean free path of 400-, 100-, and 20-keV photons in water and in a 50-g/L uranium solution. In general, transmission techniques are applicable for samples whose transmission path lengths are less than four or five mean free paths.

Equation 10-2 is useful when comparing K XRF and L XRF. For L XRF, μ is larger and more of the excitation flux interacts with the sample. For K XRF, μ is smaller and both the excitation photons and x rays are attenuated less (relative to L XRF). This attenuation difference implies that L XRF is more sensitive (more x rays produced per unit excitation flux and cross-sectional area) than K XRF. On the other hand, K XRF allows greater flexibility with respect to the choice of sample container and intervening absorbers.

10.2.4 Measurement Geometry

The choice of geometry is very important in an XRF system. Although photoelectric interactions of the excitation photons with analyte atoms are of primary interest, other interactions, particularly Compton backscatter interactions, must be considered. The energy of a Compton-scattered gamma ray is (see Section 2.3.2 of Chapter 2 and Ref. 5)

$$E' = \frac{511}{(1 - \cos\phi + 511/E)} \qquad (10\text{-}3)$$

where E′, E = scattered, incident photon energy in keV
ϕ = angle between incident and scattered photons.

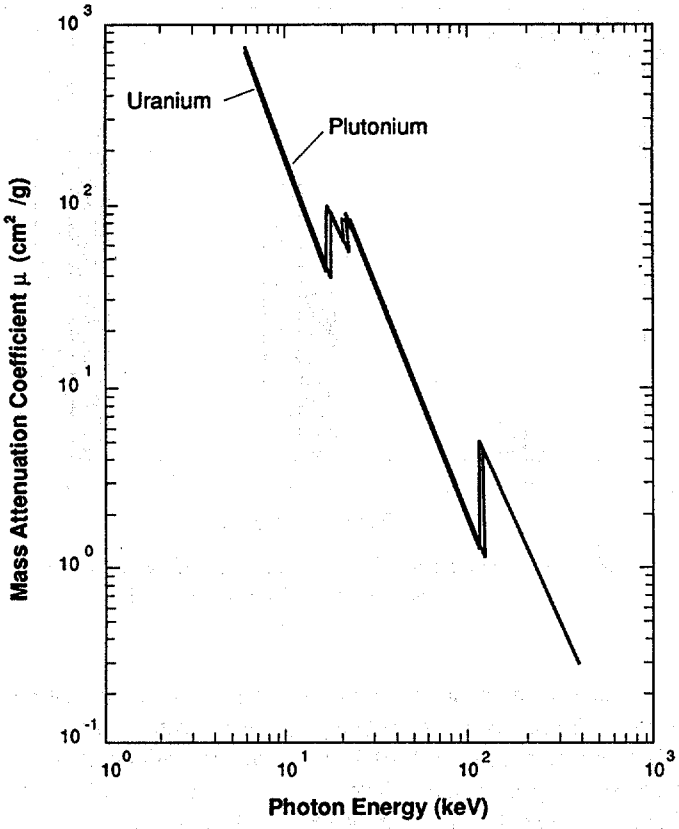

Fig. 10.6 *Mass attenuation coefficient vs energy for uranium and plutonium.*

The energy E′ is a minimum when $\phi = 180°$, and photons that have scattered at or near this angle can produce a backscatter peak in the measured spectrum. For 122-keV photons from ^{57}Co (a suitable source for K XRF of uranium or plutonium), the backscatter peak is at 82.6 keV. If the scattering angle ϕ is 90°, E′ is 98.5 keV, which is in the middle of the K x-ray spectrum from uranium and plutonium. If ^{57}Co is used as an excitation source, the measurement geometry should be arranged such that ϕ is close to 180° for most of the scattered gamma rays that reach the detector. This arrangement puts the backscatter peak and the Compton continuum of scattered photons below the characteristic x rays and minimizes the background under the x-ray photopeaks (see Figure 10.3). The annular source described later in the chapter provides this favorable geometry. For L x rays, the geometry is not as critical because E′(180°) is 20.3 keV for 22-keV silver x rays from ^{109}Cd (a good L XRF source for uranium), and the backscatter peak is above the x-ray region of interest. Scattering

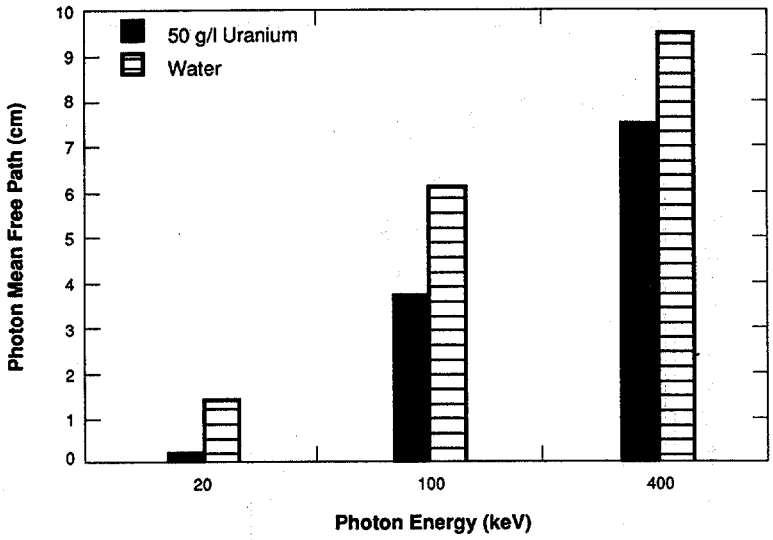

Fig. 10.7 Mean free path of 400-, 100-, and 20-keV photons in water (ρ = 1 g/cm^3) and in a 50-g/L uranium solution.

materials near the detector must be carefully controlled to minimize the magnitude of the backscatter peak. Some investigators (Ref. 6) use excitation sources with energies much higher than the binding energy of interest, thereby minimizing the scattering effects in the spectral region of the induced x rays. This approach requires higher-intensity excitation sources (by an order of magnitude or more) in order to produce sufficient x-ray activity.

The detector must be shielded from the excitation source and other background radiation to reduce deadtime and pileup losses. Detector collimation is usually necessary to limit the interference from unwanted sources. To stabilize the x-ray response, the relative positions of the source, sample, and detector must be fixed; often these components are physically connected. Figure 10.8 shows a possible geometry for a transmission-corrected XRF analysis.

10.3 TYPES OF SOURCES

Two types of sources are commonly used: discrete gamma-ray or x-ray sources and continuous sources such as x-ray generators. Each has advantages and disadvantages. The selection of a suitable source involves consideration of type, energy, and strength. It is most efficient to choose a source whose energy is above but as close as possible to the absorption edge of interest. As shown by the graph of μ vs photon energy

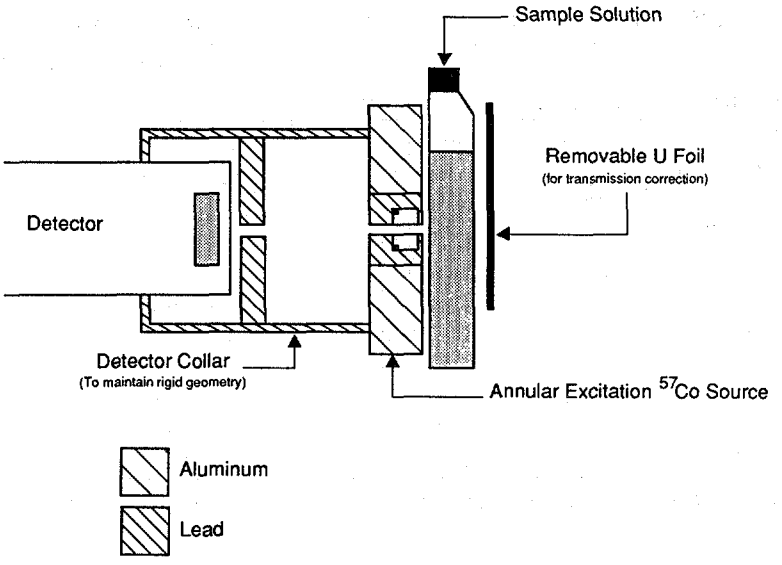

Fig. 10.8 *Cross-sectional view of geometry for a transmission-corrected assay using an annular excitation source.*

in Figure 10.6, the value of the mass attenuation coefficient is greatest just above an absorption edge.

Cobalt-57 emits a gamma ray at 122 keV, an efficient energy for K-shell ionization of either uranium or plutonium. X-ray generators are available for K XRF of uranium and plutonium, but they are too bulky for portable applications. A good discrete source for L XRF of uranium and plutonium is ^{109}Cd, which emits silver K x rays ($K_{\alpha 1}$ energy = 22 keV). X-ray generators are available that are small enough for portable applications that require photons in the 25-keV energy range.

Discrete line sources are small, extremely stable, and operationally simple, making them attractive for many XRF applications. Their major disadvantage is that they decay with time and require periodic replacement. (Two commonly used sources, ^{57}Co and ^{109}Cd, have half-lives of 272 days and 453 days, respectively.) Another disadvantage is that discrete sources cannot be turned off, causing transportation and handling difficulties. Because the source strength is often 1 mCi or greater, both personnel and detector must be carefully shielded. Table 10-2 lists some radioisotopes that can be used for XRF analysis of uranium and plutonium. The geometry of the annular source shown in Figure 10.9 is commonly used because it shields the detector from the excitation source and minimizes backscatter interference.

Table 10-2. Excitation sources suitable for uranium and plutonium assay

			Useful Emissions	
Radionuclide	Half-Life	Decay Mode	Type	Energy (keV)
^{57}Co	270 d	electron capture	gamma rays	122
			gamma rays	136
^{109}Cd	453 d	electron capture	Ag K x rays	22
^{75}Se	120 d	electron capture	gamma rays	121
			gamma rays	136
^{144}Ce	285 d	beta decay	Pr K x rays	36
			gamma rays	134
^{125}I	60 d	electron capture	Te K x rays	27
			gamma rays	35
^{147}Pm-Al	2.6 y	beta decay	continuum	12-45[a]

[a]End point of bremsstrahlung spectrum.

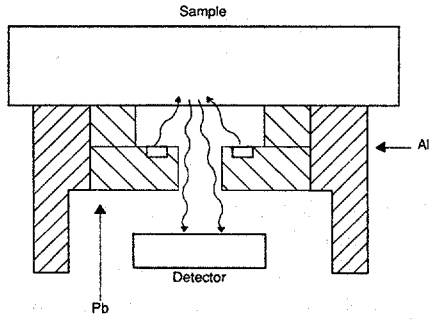

Fig. 10.9 *Annular excitation source.*

X-ray generators produce bremsstrahlung by boiling electrons off a filament and accelerating them into a target. Because they require a high-voltage supply and a means of dissipating the heat produced in the target, x-ray generators can be bulky, especially for higher operating potentials. Small generators are available that operate below 70 keV, and portable generators, with power ratings up to 50 W, are available that do not require elaborate cooling systems. For a given power rating, higher maximum operating voltage is achieved at the expense of lower available current.

The spectrum from an x-ray generator spans the energy range from the accelerating potential of the generator to the transmission cutoff of the x-ray window. The shape I(E) and total intensity (I) of this distribution is given by (Ref. 4)

$$I(E) \propto iZ(V - E)E$$
$$I \propto iZV^2 \qquad (10\text{-}4)$$

where i = tube current
V = operating voltage
Z = atomic number of target.

Figure 10.10 shows the output spectrum from an x-ray generator. In addition to the continuous spectrum, the characteristic x rays of the target material are produced. These x rays may cause an interference, which can be removed with filters. The filter chosen should have an absorption edge just below the energy to be attenuated.

X-ray generators can be switched on and off, and their energy distribution and intensity can be varied as desired. They typically provide a more intense source of photons than radioisotopic sources ($\sim 10^{12}$ photons/s or greater). However, their flexibility is possible only at the expense of simplicity and compactness. Because an x-ray generator is an electrical device, system failures and maintenance problems are possible concerns. The assay precision is dictated by the stability of the x-ray tube. Modern generators exhibit less than 0.1% fluctuation for short-term stability and 0.2 to 0.3% for long-term stability. Figure 10.11 shows two different portable x-ray generators.

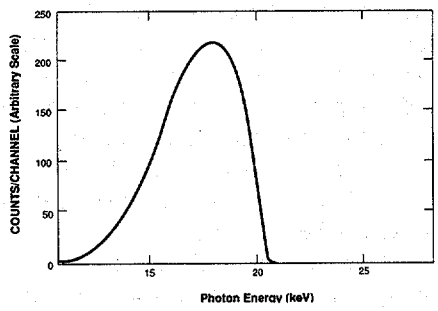

Fig. 10.10 *Typical x-ray generator spectrum. The generator target is tungsten and the operating potential is 20.4 kV.*

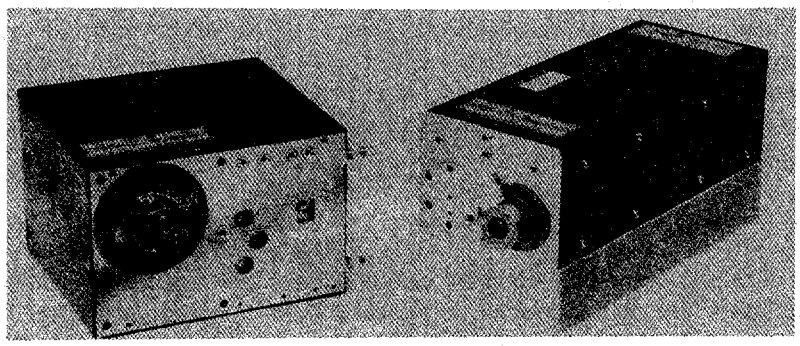

Fig. 10.11 *Portable x-ray generators.*

Other sources may be used for XRF. A secondary fluorescent source uses a primary photon source to excite the characteristic x rays of a target, and the target x rays are used to excite the sample to be analyzed. The primary excitation source can be discrete or continuous. This scheme can produce a great variety of monoenergetic excitation photons, depending on the target material. The major drawback is the need for a high-intensity primary source. If the primary source is a radioisotope, radiation safety may be an important concern. It is possible to make a bremsstrahlung source using a radioisotope rather than an x-ray generator. Such a source consists of a beta-decaying isotope mixed with a target material (for example, ^{147}Pm-Al, with aluminum being the target material).

10.4 CORRECTION FOR SAMPLE ATTENUATION

10.4.1 Effects of Sample Attenuation

As in passive gamma-ray assays, sample attenuation is a fundamental limitation to the accuracy of XRF analysis. Attenuation corrections are required for the x rays leaving the sample and also for the gamma rays or x rays from the excitation source. X-ray fluorescence analysis is unsuitable for large, solid samples, because the attenuation is too large to be accurately treated with any correction procedure. For example, the mean free path of 122-keV gamma rays in uranium metal is approximately 0.013 cm. The low penetrability of this radiation means that XRF can be accurately used only if the sample is smooth and homogeneous. This limitation is even more true for L XRF using 22-keV photons. X-ray fluorescence can be used to accurately assay dilute uranium solutions because the mean free path of photons in water is approximately 6.4 cm at 122 keV and 1.7 cm at 22 keV. Because the excitation source energy is above the absorption edge and the energies of the characteristic x rays are just below the absorption edge, the attenuation of the excitation radiation is higher and determines the range of sample thickness that can be accurately assayed. Figure 10.12 plots the mean free path of 122-keV gamma rays as a function of uranium concentration (uranyl nitrate in 4-M nitric acid).

Attenuation considerations also affect the choice of sample containers. Because the K x rays of uranium and plutonium are in the 100-keV range, metal containers can be tolerated, and K XRF can be applied to in-line measurements. L x rays, however, are severely attenuated by even thin metal containers and can only be measured in low-Z containers, such as plastic or glass.

10.4.2 General Assay Equation

For quantitative analysis, the x-ray emission rate must be related to the element concentration. The desired relation, as presented in Section 5.4.1 of Chapter 5, is

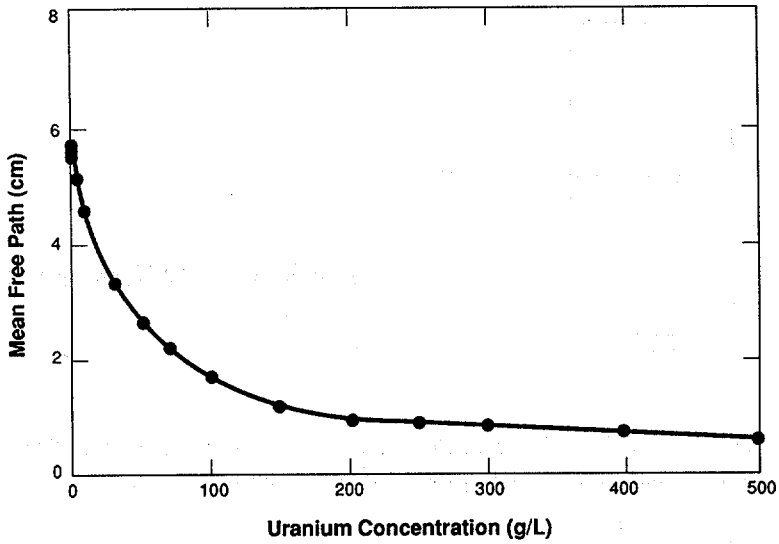

Fig. 10.12 *The 122-keV photon mean free path vs uranium concentration (uranyl nitrate in 4-M nitric acid).*

$$\rho = \frac{RR \times CF(RL) \times CF(AT)}{K} \tag{10-5}$$

where ρ = element concentration
RR = raw rate of x-ray detection
CF(RL) = correction factor for rate-related losses
CF(AT) = correction factor for attenuation
K = calibration constant.

CF(RL) can be determined using either pulser or radioisotope normalization (see Section 5.4 of Chapter 5). The attenuation correction has two parts, one for excitation radiation and one for fluoresced x rays.

Consider a far-field measurement geometry where the sample is approximated by a slab and the excitation source is monoenergetic (see Figure 10.13). The flux F_γ of excitation photons at a depth x in the sample is given by

$$F_\gamma = I_\gamma \exp(-\mu^\gamma X/\cos\phi) \ . \tag{10-6}$$

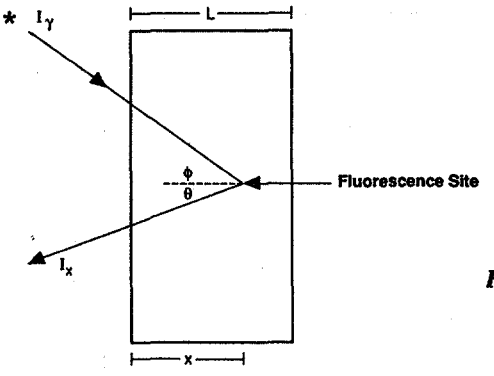

Fig. 10.13 General XRF slab geometry.

The variables in Equation 10-6 through 10-10 are defined in Table 10-3. The number of excitation photons that interact in the volume dx and create a $K_{\alpha 1}$ x ray is

$$F_x\, dx = F_\gamma \tau \rho \omega B \frac{dx}{\cos\phi} \quad . \tag{10-7}$$

The fluoresced x rays are attenuated in the sample according to

$$F_x(\text{out}) = F_x \exp(-\mu^x X/\cos\theta) \quad . \tag{10-8}$$

Combining and integrating Equations 10-6 through 10-8 yields the following expression for the x-ray rate at the detector surface:

$$I_x = \frac{I_\gamma \tau \rho \omega B \Omega}{4\pi[(\cos\theta/\cos\phi)\mu^\gamma + \mu^x]} \left\{1 - \exp\left[-\left(\frac{\mu^\gamma}{\cos\phi} + \frac{\mu^x}{\cos\theta}\right) L\right]\right\}. \tag{10-9}$$

The factor $(\Omega/4\pi)\ \cos\phi/\cos\theta$ has been added for normalization. If an x-ray generator is used as the excitation source, Equation 10-9 must be integrated from the absorption edge to the maximum energy of the generator.

When the sample is infinitely thick for the radiation of interest, Equation 10-9 becomes

$$I_x = \frac{I_\gamma\ \tau \rho \omega B \Omega}{4\pi[(\cos\theta/\cos\phi)\mu^\gamma + \mu^x]} \quad . \tag{10-10}$$

This equation is similar to that of the enrichment meter (see Chapter 7). The result is very important for XRF analysis because it implies that the x-ray rate is directly proportional to the concentration of the fluoresced element.

In plutonium and highly enriched uranium materials, the self-excitation of x rays by the passive gamma rays can complicate the assay. For mixed uranium/plutonium materials, the dominant signals are passive x rays from the alpha decay of plutonium. When the excitation source can fluoresce both plutonium and uranium (as can ^{57}Co and ^{109}Cd), additional uranium fluorescence is caused by the plutonium x rays. A separate passive count is usually required to correct for this interference.

Table 10-3. Variables in Equations 10-6 through 10-10

I_0	excitation flux at sample surface
τ	photoelectric cross section, K shell, γ energy
ρ	concentration of element s
ω	K fluorescence yield
B	branching ratio for $K_{\alpha 1}$
Ω	detector solid angle
$\mu^{\gamma} = \sum \mu_i^{\gamma} \rho_i$	linear attenuation coefficient, γ energy, element i
$\mu^{x} = \sum \mu_i^{x} \rho_i$	linear attenuation coefficient, x energy, element i
ϕ	incident angle of excitation
Θ	exiting angle of x ray
L	slab thickness

10.4.3 Attenuation Correction Methods

The most effective XRF methods account for sample attenuation. The simplest approach uses calibration curves derived from chemically similar standards. The method is effective only if the standards are well characterized, match the samples chemically, and span the concentration range to be assayed in sufficient numbers to define the calibration curve. Changes in matrix composition may require recalibration with new standards.

A procedure that is less sensitive to matrix variation is the transmission-corrected assay (Refs. 7 through 9) in which a transmission measurement is made for each sample to correct for attenuation. Consider the attenuation correction factor for the situation shown in Figure 10.13 (assume that $\Theta = 0$). The expression for CF(AT) has the functional form for a slab that was discussed in Chapter 6:

$$CF(AT) = \frac{-\ln \alpha}{1 - \alpha} \tag{10-11}$$

where

$$\alpha = \exp\left[-\left(\frac{\mu^{\gamma}}{\cos\phi} + \mu^{x} \right) L \right] .$$

A measurement of the transmissions of the excitation and the fluoresced x rays can be used to determine α. For this method, a foil of the element being measured is placed behind the sample and the induced x-ray signal is measured with and without the sample. An additional measurement (see Figure 10.14) is made with the sample only (no foil), and α is computed from

$$\alpha = \frac{I_T - I_S}{I_0} \tag{10-12}$$

where I_T = fluoresced x-ray intensity with foil plus sample
I_S = fluoresced x-ray intensity with sample only
I_0 = fluoresced x-ray intensity with foil only.

This measurement includes the attenuation of the excitation source and of the induced x-ray signal. Although there are advantages to using the same element in the transmission foil as that being assayed, other elements can be used if their characteristic x rays are sufficiently close to those of the assay element. For example, thorium metal has been used successfully for the measurement of uranium solutions.

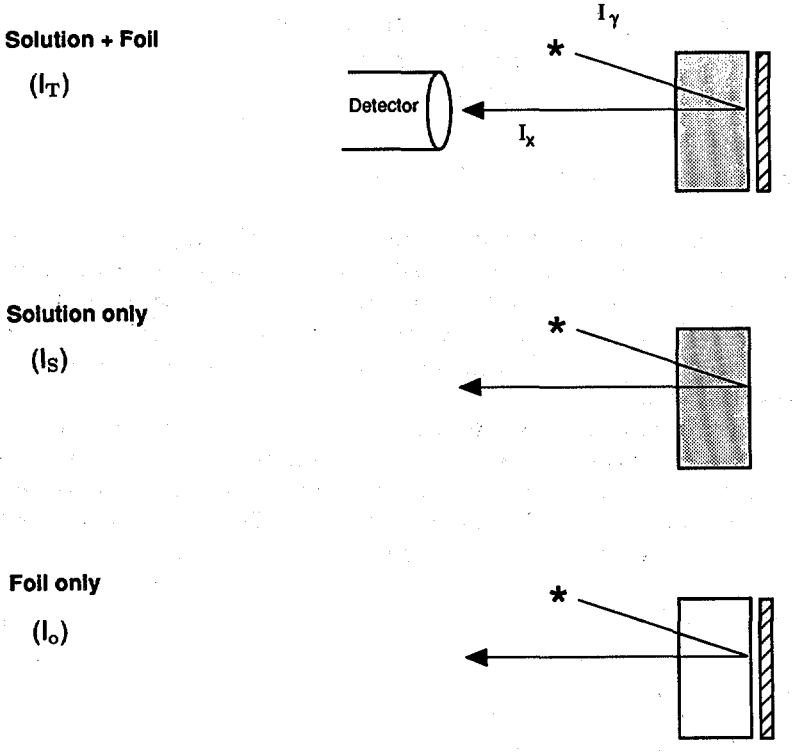

Fig. 10.14 *Explanation of the three measurements required to determine the transmission for XRF assay of uranium solutions.*

A suitable number of standards is needed to evaluate the calibration constant K in Equation 10-5. Equations 10-11 and 10-12 are exact only for a far-field geometry, and most XRF measurements are made in a near-field geometry. Therefore, even with rate and sample attenuation corrections, it is important to use several standards to evaluate the calibration constant K.

10.5 APPLICATIONS AND INSTRUMENTATION

Instrumentation used in XRF analysis is similar to that of other gamma-ray assay systems: detector, associated electronics, multichannel analyzer, and excitation source. This instrumentation is discussed in detail in Chapter 4.

XRF analysis has been used in analytical chemistry laboratories for many years. In most cases, an x-ray generator is used rather than a radioisotope as an excitation source. Low- to intermediate-Z elements are measured, and sample preparation is a key factor in the analysis. Many techniques require that the sample be homogenized and pressed prior to analysis. When the sample can be modified to optimize the assay, XRF analysis is very sensitive. Short count times (<1000 s) can yield accurate and precise data, with sensitivities in the nanogram range (Ref. 1). Complete XRF systems are available commercially.

Several XRF measurement techniques are used for materials containing uranium or plutonium. John et al. (Ref. 10) used a ^{57}Co source to excite uranium x rays in solutions and simultaneously observed the 185.7-keV gamma ray from ^{235}U as a measure of enrichment. The ratio of the fluoresced x-ray emission to the 185.7-keV gamma-ray intensity was found to be independent of uranium concentration in the 8- to 20-g/L range for enrichments of 0.4 to 4.5% ^{235}U. Accuracies of better than 1% were reported.

Rowson and Hontzeas (Ref. 11) proposed a Compton-scattering-based correction for sample attenuation to measure uranium ores. An annular 50-mCi ^{241}Am source was used to excite characteristic x rays from a molybdenum foil (~17.4 keV), which can only excite the L_{III} subshell in uranium. This considerably simplifies the L x-ray spectrum. Matrix corrections were determined from the ratio of the molybdenum K_α backscatter to the uranium L_α x rays. Canada and Hsue (Ref. 12) give a good theoretical description of this method and suggest an improvement that involves additional ratios using the K_β or L_β lines to further minimize matrix effects.

Baba and Muto (Ref. 13) used an x-ray generator to excite the L x-ray spectrum of uranium- and plutonium-bearing solutions. An internal standard was used to determine the matrix attenuation correction. A known and constant amount of lead nitrate was added to all solutions and the uranium or plutonium L_α x-ray activity was normalized to the rate of the lead L_α x ray. A linear calibration (to within 1% for uranium and 2% for plutonium) was obtained for 200-s measurements. The solution concentrations ranged from 0.1 to 200 g/L of uranium and up to 50 g/L of plutonium. Mixed uranium/plutonium solutions were also measured.

Karamanova (Ref. 14) investigated the use of beta-particle-induced XRF in addition to gamma-ray excitation for K XRF analysis of uranium and mixed uranium/thorium oxides. A ^{57}Co source was used for gamma-ray excitation, and a ^{90}Sr-^{90}Y source was used for beta-particle-induced fluorescence. Since the attenuation cross sections of the matrix and the heavy element are similar for beta-particle excitation, the volume of sample is essentially constant and the net x-ray signal is proportional to the concentration of the element being assayed. Samples with uranium concentrations of 0.5 to 88% were measured with precisions of 0.1%.

Several investigators have measured reprocessing plant solutions. These solutions can contain fission products and have high U/Pu ratios, making them very difficult to assay by passive techniques. They require either extensive chemical separations or a sensitive technique such as XRF. Pickles and Cate (Ref. 15) employed XRF using an x-ray generator. Samples with U/Pu ratios of up to 400 and fission product activities of 2 Ci/g were analyzed with a precision of 1% and an accuracy of 2% in the mass range of 1 to 58 μg using a 10-min count. The samples were evaporated onto a thin polycarbonate film to minimize sample attenuation. Figure 10.15 shows the instrumental configuration. The sample chamber contained titanium sheets on either side of the sample mount. X rays from the titanium provided a rate-loss correction. A magnetic beta-particle trap and a lead collimator were employed to reduce the passive signal at the detector.

Camp et al. (Refs. 16 and 17) use a ^{57}Co excitation source to fluoresce K x rays from uranium and plutonium in product streams at reprocessing plants. Total heavy element concentrations of 1 to 200 g/L are assayed using a nonlinear polynomial calibration. The self-attenuation correction uses the incoherently scattered 122-keV gamma rays from ^{57}Co (Ref. 16) or an actual transmission measurement using the 122-keV gamma ray (Ref. 17). In samples containing both uranium and plutonium, a passive count is made to correct for passive x-ray emission.

Andrew et al. (Ref. 18) investigated the feasibility of measuring uranium and uranium/thorium solutions with uranium concentrations of 10 to 540 g/L. For solutions containing both uranium and thorium, errors in the U/Th ratio were 0.4%. Uncertainties in concentration measurements were 0.5% for single element solutions and 1% for mixed solutions. This work was extended to uranium/plutonium solutions from reprocessing plants (Refs. 19 and 20). Uranium and plutonium solutions in the range of 1 to 10 g/L with a fission product activity of 100 μCi/mL were measured by tube-excited K XRF. The data analysis was similar to that used for uranium/thorium solutions, and the authors suggested combining K XRF and K-edge densitometry to obtain absolute element concentrations.

Ottmar et al. (Refs. 21 and 22) investigated the combination of K XRF and K-edge densitometry using an x-ray generator. The two techniques are complementary and produce a measurement system with a wide dynamic range. Light-water-reactor dissolver solutions with activities of ~100 Ci/L and U/Pu ratios of ~100 have been accurately measured with this system. The major component, uranium (~200 g/L), is determined using absorption-edge densitometry, whereas the U/Pu ratio is determined

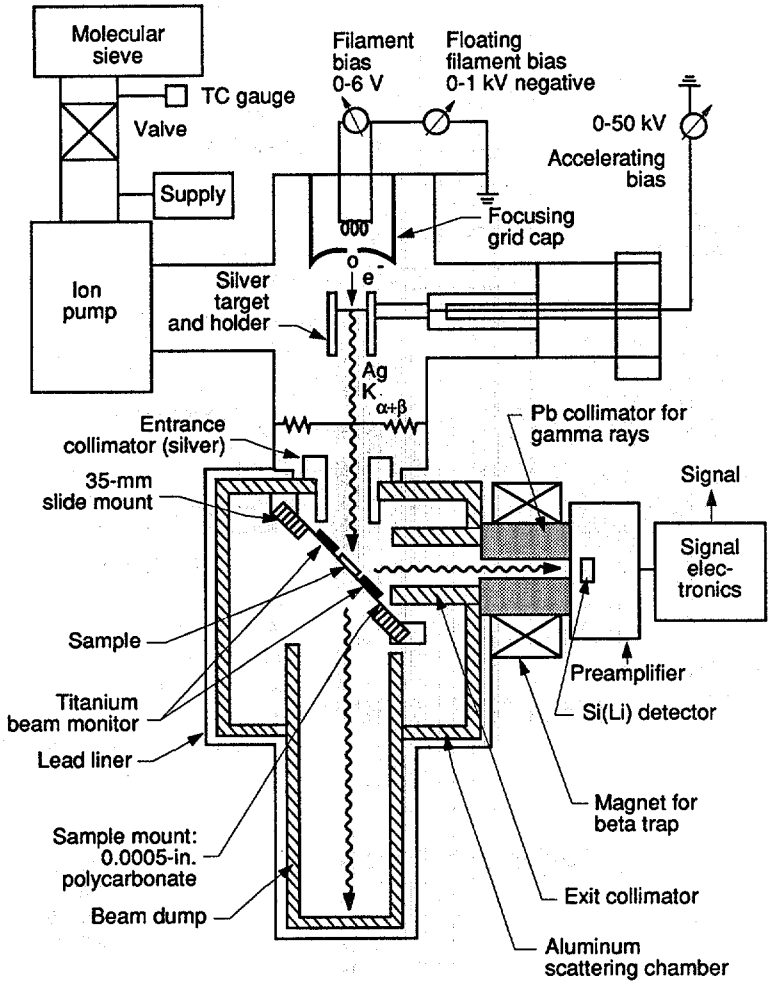

Fig. 10.15 *Schematic drawing of system used by Pickles and Cate (Ref. 15).*

by XRF. Precisions of 0.25% for the uranium concentration and 1% for the U/Pu ratio are obtained in 1000-s count times. Two sample cells are employed: a 2-cm glass cuvette (whose dimensions are known to ± 2 μm) for the densitometry measurement, and a 1-cm-diam polyethylene vial for the XRF measurement. The XRF measurement is made at a back angle of $\sim 157°$ in order to maximize the signal-to-background ratio. Figure 10.16 shows this hybrid system.

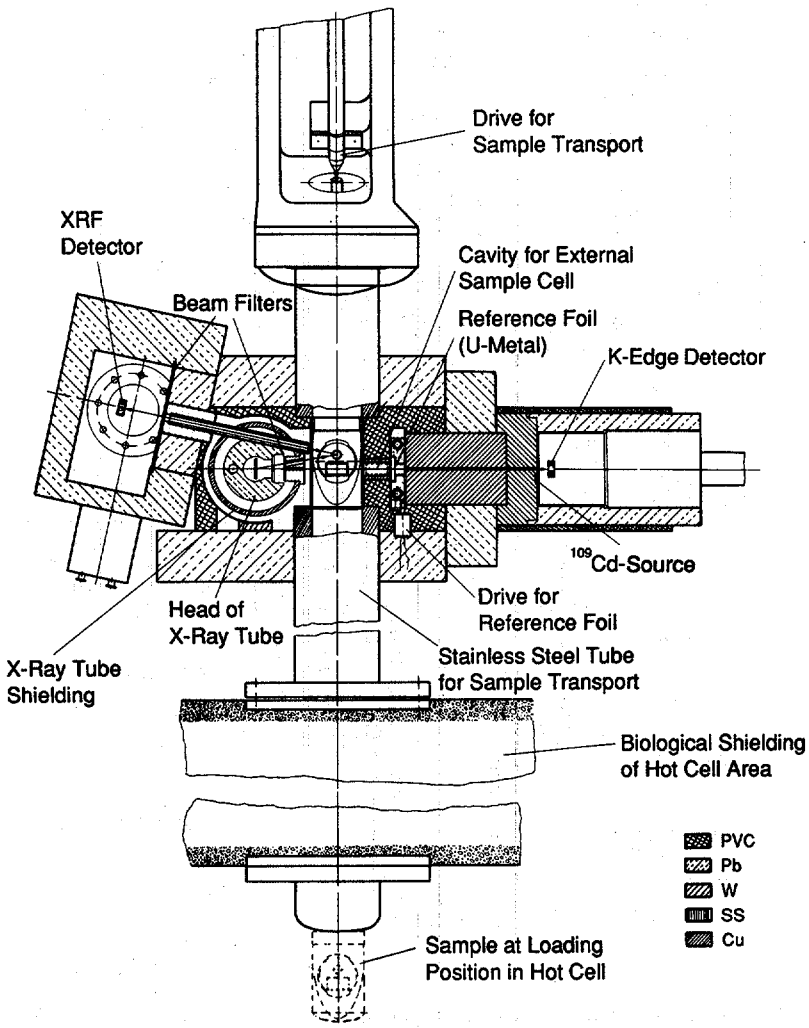

Fig. 10.16 *Schematic drawing of hybrid K-edge/K XRF system (Ref. 21). (Courtesy of H. Ottmar).*

Lambert et al. (Ref. 23) employed secondary-excitation L XRF to measure the U/Pu ratio in mixed-oxide fuel pellets. A pellet with 25% PuO_2 and 75% UO_2 gave a precision of about 0.5% in a 3-min count time. The desired x rays were excited using selectable secondary target foils (rhodium). The method requires good sample homogeneity because the portion of sample analyzed (~30-μm depth of analysis) is relatively small.

REFERENCES

1. E. P. Bertin, *Principles and Practice of X-Ray Spectrometric Analysis* (Plenum Press, New York, 1975).

2. R. Jenkins, R. W. Gould, and D. Gedcke, *Quantitative X-Ray Spectrometry* (Marcel Dekker, Inc., New York, 1981).

3. R. Tertian and F. Claisse, *Principles of Quantitative X-Ray Fluorescence Analysis* (Heyden & Son, Inc., Philadelphia, Pennsylvania, 1982).

4. R. Woldseth, *All You Ever Wanted to Know About XES* (Kevex Corp., Burlingame, California, 1973).

5. G. F. Knoll, *Radiation Detection and Measurement* (John Wiley & Sons, Inc., New York, 1979), p. 310.

6. P. Martinelli, "Possibilities of Plutonium Analysis by Means of X-Ray Fluorescence with an Iridium-192 Radioactive Source," *Analysis* 8 (10), 499–504 (1980).

7. R. Strittmatter, M. Baker, and P. Russo, "Uranium Solution Assay by Transmission-Corrected X-Ray Fluorescence," in "Nuclear Safeguards Research and Development Program Status Report, May–August 1978," Los Alamos Scientific Laboratory report LA-7616-PR (1979), pp. 23–24.

8. T. R. Canada, D. C. Camp, and W. D. Ruhter, "Single-Energy Transmission-Corrected Energy-Dispersive XRF for SNM-Bearing Solutions," Los Alamos National Laboratory document LA-UR-82-557.

9. P. Russo, M. P. Baker, and T. R. Canada, "Uranium-Plutonium Solution Assay by Transmission-Corrected X-Ray Fluorescence," in "Nuclear Safeguards Research and Development Program Status Report, September–December, 1977," Los Alamos Scientific Laboratory report LA-7211-PR (1978), pp. 22–28.

10. J. John, F. Sebesta, and J. Sedlacek, "Determination of Uranium Isotopic Composition in Aqueous Solutions by Combined Gamma Spectrometry and X-Ray Fluorescence," *Journal of Radioanalytical Chemistry* 78 (2), 367–374 (1983).

11. J. W. Rowson and S. A. Hontzeas, "Radioisotopic X-Ray Analysis of Uranium Ores Using Compton Scattering for Matrix Correction," *Canadian Journal of Spectroscopy* 22 (1), 24–30 (1977).

12. T. R. Canada and S.-T. Hsue, "A Note on the Assay of Special Nuclear Materials in Solution by X-Ray Fluorescence," *Nuclear Materials Management* XI (2), 91 (1982).

13. Y. Baba and H. Muto, "Determination of Uranium and Plutonium in Solution by Energy-Dispersive X-Ray Fluorescence Analysis," *Bunseki Kagaku* 32, T99–T104 (1983).

14. J. Karamanova, "Development of an Express NDA Technique (using radioisotopic sources) for the Concentration Measurements of Nuclear Materials, 1 November 1974-30 June 1977," International Atomic Energy Agency report IAEA-R-1557R (1977).

15. W. L. Pickles and J. L. Cate, Jr., "Quantitative Nondispersive X-Ray Fluorescence Analysis of Highly Radioactive Samples for Uranium and Plutonium Concentrations," Lawrence Livermore Laboratory report UCRL-7417 (1973).

16. D. C. Camp and W. D. Ruhter, "Nondestructive, Energy-Dispersive X-Ray Fluorescence Analysis of Product Stream Concentrations from Reprocessed Nuclear Fuels," in *Proc. American Nuclear Society Topical Conference on Measurement Technology for Safeguards and Materials Control*, Kiawah Island, South Carolina, November 26–28, 1979 (National Bureau of Standards, Washington, DC, 1980), p. 584.

17. D. C. Camp, W. D. Ruhter, and K. W. MacMurdo, "Determination of Actinide Process- and Product-Stream Concentrations Off-line or At-line by Energy-Dispersive X-Ray Fluorescence Analysis," in *Proc. Third Annual Symposium on Safeguards and Nuclear Materials Management*, Karlsruhe, Federal Republic of Germany, May 6-8, 1981 (European Safeguards Research and Development Association, Brussels, Belgium, 1981), p. 155.

18. G. Andrew, B. L. Taylor, and B. Metcalfe, "Estimation of Special Nuclear Materials in Solution by K X-ray Fluorescence and Absorption Edge Densitometry," United Kingdom Atomic Energy Authority report AERE-R9707 (1980).

19. G. Andrew and B. L. Taylor, "The Measurement of Pu and U in Reprocessing Plant Solutions by Tube-Excited K X-Ray Fluorescence," United Kingdom Atomic Energy Authority report AERE-R9864 (1980).

20. G. Andrew and B. L. Taylor, "The Feasibility of Using K-XRF for the On-line Measurement of Pu/U Ratios of Highly Active Dissolver Solutions," United Kingdom Atomic Energy Authority report AERE-M3134 (1980).

21. H. Ottmar, H. Eberle, P. Matussek, and I. Michel-Piper, "Qualification of K-Absorption Edge Densitometry for Applications in International Safeguards," International Atomic Energy report IAEA-SM-260/34 (1982).

22. H. Ottmar, H. Eberle, P. Matussek, and I. Michel-Piper, "How to Simplify the Analytics for Input-Output Accountabilty Measurements in a Reprocessing Plant," Kernforschungszentrum Karlsruhe report KfK 4012 (1986).

23. M. C. Lambert, M. W. Goheen, M. W. Urie, and N. Wynhoff, "An Automated X-Ray Spectrometer for Mixed-Oxide Pellets," Hanford Engineering Development Laboratory report HEDL-SA1492 (1978).